INTERNATIONAL JOURNAL FOR NUMERICAL METHODS IN FLUIDS, VOL. 22, 569–580 (1996)

NUMERICAL SOLUTIONS OF ONE-DIMENSIONAL MHD EQUATIONS BY A FLUCTUATION APPROACH

NECDET ASLAN

Marmara University, Fen.-Ed., Physics Department, Göztepe Istanbul, Turkey

SUMMARY

In this paper a higher-order Godunov method for one-dimensional solutions of the ideal MHD (magneto-hydrodynamics) equations is presented. The method uses a fluctuation approach and includes a new sonic fix and a new Roe averaging. After a short introduction the MHD equations in conservative form are given. The flux is rearranged such that the eigenstructure is not changed. This rearrangement allows full Roe averaging for any value of adiabatic index (contrary to Brio and Wu's conclusion). A new procedure to get Roe—averaged MHD fields at the interfaces between left and right states is then presented and some useful identities are given. Next the second-order-limited fluctuation approach is presented in full detail. The new sonic fix for MHD and the procedure for applying this fix to the sonic points are then given in detail. Numerical results obtained with the described method are presented. Finally, conclusions are given.

KEY WORDS magnetohydrodynamics; Godunov; upwind; conservative; plasma; fusion

1. INTRODUCTION

Conservative numerical schemes based on higher-order Godunov methods have been effectively used for computing discontinuous solutions of hyperbolic systems of equations. Several examples of the solution of equations of hydrodynamics by such schemes are available. Most of these schemes suffer from sonic points at which characteristic speeds vanish. Several examples of fixing the solution at such points are also available in the literature.[4–6]

Finite volume and fluctuation approaches based on higher-order Godunov schemes are two of the favourite conservative methods. In the finite volume approach the local solution that changes in time is obtained by means of a numerical flux function evaluated at the interfaces between mesh points. The fluctuation approach is based on obtaining this local solution via the local imbalance of fluxes. This approach is more sensitive to degeneracy fixes and implementing the boundary conditions with it is rather simple.

First numerical results for the solution of MHD equations were published by Brio and Wu,[7] who solved the one-dimensional ideal MHD equations using Roe's method. They showed that compound waves (a slow shock and an attached rarefaction wave) can exist in MHD. Zachary and Colella[8] applied a method originally developed by Bell *et al.*[9] to the ideal MHD equations and obtained results that were in good agreement with those reported by Brio and Wu. One of the test problems Brio and Wu presented included a strong sonic point where they used a type of Harten fix. Zachary and Colella used structure coefficients to detect and fix these sonic points. In this work, Roe's fluctuation approach is used for solving the ideal MHD equations numerically in one dimension. A new sonic fix which eliminates the unphysical expansion shock and a new Roe averaging which guarantees that the Rankine–Hugoniot conditions are satisfied at the interfaces between grid points are presented.[10]

CCC 0271–2091/96/070569–12

Received June 1994
Revised November 1994

2. BASIC EQUATIONS

The one-dimensional ideal MHD equations in conservative form are written as

$$\frac{\partial U}{\partial t}+\frac{\partial F(U)}{\partial x}=S_x(\vec{U}), \tag{1}$$

where U is the state, $F(U)$ is the flux and $S_x(\vec{U})$ is the source vector which are explicitly given by

$$\frac{\partial}{\partial t}\begin{bmatrix}\rho\\ \rho V_x\\ \rho V_y\\ \rho V_z\\ B_x\\ B_y\\ B_z\\ E_\perp\end{bmatrix}+\frac{\partial}{\partial x}\begin{bmatrix}\rho V_x\\ \rho V_x^2+P_\perp^*\\ \rho V_xV_y-B_xB_y/4\pi\\ \rho V_xV_z-B_xB_z/4\pi\\ 0\\ V_xB_y-B_xV_y\\ V_xB_z-B_xV_z\\ (E_\perp+P_\perp^*)V_x-(B_x/4\pi)\vec{V}_\perp\cdot\vec{B}_\perp\end{bmatrix}=\begin{bmatrix}0\\ (\partial/\partial x)(B_x^2/4\pi)\\ 0\\ 0\\ 0\\ 0\\ 0\\ 0\end{bmatrix}. \tag{2}$$

Here ρ is the density, $\vec{V}$ is the velocity, $\vec{B}$ is the magnetic field and $E_\perp$ and $P_\perp^*$ are the total perpendicular energy and total perpendicular pressure respectively,

$$E_\perp=\tfrac{1}{2}\rho V^2+\frac{B_\perp^2}{8\pi}+\rho e, \qquad P_\perp^*=P+\frac{B_\perp^2}{8\pi}, \tag{3}$$

where $V^2=V_x^2+V_y^2+V_z^2, B_\perp^2=B_y^2+B_z^2, a=\sqrt{(\gamma P/\rho)}$ is the speed of sound and e is the internal energy related to the scalar pressure P by the equation of state $e=(P/\rho)/(\gamma-1)$.

When an operator-splitting scheme is used for two-dimensional problems, $E_\perp$ has to be redefined in each direction (see Reference 8 for a similar procedure). When curvilinear geometries are considered, the sourse vector must be split very carefully (see, e.g. Reference 10). Equation (2) are written in this way because there are a few advantages. The first advantage is that the eigensystem of the flux Jacobian[7,8,10] remains unchanged. Secondly, full or partial Roe averaging for any value of adiabatic index γ becomes possible (contrary to Brio and Wu's conclusion[7]). Note that (for hydrodynamics) full Roe averaging of the density, velocity and pressure fields at the interfaces between meshes is achieved by enforcing that the Rankine–Hugoniot (R–H) conditions be satisfied exactly. In MHD, Roe averaging of the density and velocity fields remains the same as in hydrodynamics. It is shown for the first time in this paper that Roe averaging is also feasible for the pressure and the magnetic field if its parallel component (*i.e.* B_x in one dimension) does not vary in space. If it varies in space, simple arithmetic averaging can be used, this is called 'partial Roe averaging' in this work. The final advantage is that the problems arising from the $\vec{\nabla}\cdot\vec{B}=0$ conditions are mostly eliminated (which will be the subject of subsequent publications).

In Roe's fluctuation approach[6] the gradients of U and F are given by the following eigenvector decompositions in which the characteristic waves are decomposed into k simple wave contributions:

$$\Delta U=\sum_k \tilde{\alpha}_k\tilde{r}_k, \tag{4}$$

$$\Delta F=\sum_k \tilde{\alpha}_k\tilde{\lambda}_k\tilde{r}_k, \tag{5}$$

$$-\Delta xS_x=\sum_k \tilde{\beta}_k\tilde{r}_k, \tag{6}$$

where $\tilde{\lambda}_k$ and $\tilde{r}_k$ are the eigenvalues and right eigenvectors of the Jacobian matrix respectively,

$\tilde{A}_u = \partial F/\partial U$, $\tilde{\alpha}_k$ and $\tilde{\beta}_k$ are the wave and source strengths and the 'tildes' above the quantities represent their Roe-averaged values at the interfaces between mesh points.

3. ROE AVERAGING

The importance of Roe averaging[2,11] is that it gives the fields at the interfaces between grid points in such a way that the R–H jump conditions are satisfied. According to Brio and Wu,[7] Roe averaging is not feasible for the ideal MHD equations unless $\gamma = 2$. However, it is shown in this section that Roe averaging of the density and velocity fields is feasible for any value of γ and that Roe averaging of the magnetic field and pressure is feasible only for a constant parallel magnetic field. Whenever the parallel field changes in space, arithmetic averaging can be used, which results in spreading the shocks and discontinuities. The procedure for finding Roe–averaged quantities is equivalent to seeking an approximation for averaged Jacobian ($\tilde{A} = \partial F/\partial U$) with eigenvalues $\tilde{\lambda}_k$ and eigenvectors $\tilde{r}_k$. This approach is used by Glaister[12] and is an alternative to the approach used by Brio and Wu.[7] Assuming the eigenvectors given in Reference 10, the procedure starts with writing out equation (4) and (5) explicitly:

$$\Delta[\rho] = \tilde{\rho}\tilde{\alpha}_f(\tilde{\alpha}_1 + \tilde{\alpha}_7) + \frac{\tilde{\rho}\tilde{U}_f}{\tilde{a}}\tilde{\alpha}_s(\tilde{\alpha}_5 + \tilde{\alpha}_3) + \tilde{\rho}\tilde{\alpha}_4. \tag{7}$$

$$\Delta[V_x] = \tilde{\alpha}_f\tilde{U}_f(\tilde{\alpha}_7 - \tilde{\alpha}_1) + \tilde{U}_A\tilde{\alpha}_s(\tilde{\alpha}_5 - \tilde{\alpha}_3), \tag{8}$$

$$\Delta[V_y] = -\tilde{U}_A\tilde{\alpha}_s\tilde{\beta}_y S(\tilde{\alpha}_7 - \tilde{\alpha}_1) + \tilde{U}_f\tilde{\alpha}_f\tilde{\beta}_y S(\tilde{\alpha}_5 - \tilde{\alpha}_3) - \frac{\tilde{\beta}_z}{4\pi\tilde{\rho}}(\tilde{\alpha}_6 - \tilde{\alpha}_2), \tag{9}$$

$$\Delta[V_z] = -\tilde{U}_A\tilde{\alpha}_s\tilde{\beta}_z S(\tilde{\alpha}_7 - \tilde{\alpha}_1) + \tilde{U}_f\tilde{\alpha}_f\tilde{\beta}_z S(\tilde{\alpha}_5 - \tilde{\alpha}_3) - \frac{\tilde{\beta}_y}{4\pi\tilde{\rho}}(\tilde{\alpha}_6 - \tilde{\alpha}_2). \tag{10}$$

Notice that equations (8)–(10) are obtained by using $\Delta[\rho]$ in $\Delta[\rho V_x], \Delta[\rho V_y]$ and $\Delta[\rho V_z]$ respectively.

$$\Delta[B_y] = \tilde{U}_f\tilde{\alpha}_5\tilde{\beta}_y\sqrt{(4\pi\tilde{\rho})}(\tilde{\alpha}_7 + \tilde{\alpha}_1) - \tilde{a}\tilde{\alpha}_f\tilde{\beta}_y\sqrt{(4\pi\tilde{\rho})}(\tilde{\alpha}_5 + \tilde{\alpha}_3) + \frac{\tilde{\beta}_z S}{\sqrt{(4\pi\tilde{\rho})}}(\tilde{\alpha}_6 + \tilde{\alpha}_2), \tag{11}$$

$$\Delta[B_z] = \tilde{U}_f\tilde{\alpha}_s\tilde{\beta}_z\sqrt{(4\pi\tilde{\rho})}(\tilde{\alpha}_7 + \tilde{\alpha}_1) - \tilde{a}\tilde{\alpha}_f\tilde{\beta}_z\sqrt{(4\pi\tilde{\rho})}(\tilde{\alpha}_5 + \tilde{\alpha}_3) - \frac{\tilde{\beta}_y S}{\sqrt{(4\pi\tilde{\rho})}}(\tilde{\alpha}_6 + \tilde{\alpha}_2), \tag{12}$$

$$\Delta\left[\frac{P}{\gamma - 1} + \frac{B^2}{8\pi}\right] = \frac{\tilde{\rho}\tilde{U}_f\tilde{\alpha}_s}{\tilde{a}}(\tilde{U}_s^2 - \gamma'\tilde{a}^2)(\tilde{\alpha}_5 + \tilde{\alpha}_3) + \tilde{\rho}\tilde{\alpha}_f(\tilde{U}_f^2 - \gamma'\tilde{a}^2)(\tilde{\alpha}_7 + \tilde{\alpha}_1). \tag{13}$$

Note that equation (13) leads to

$$\Delta[P] = \tilde{\rho}\tilde{U}_f\tilde{\alpha}_s\tilde{a}(\tilde{\alpha}_5 + \tilde{\alpha}_3) + \tilde{\rho}\tilde{\alpha}_f\tilde{U}_f^2(\tilde{\alpha}_7 + \tilde{\alpha}_1), \tag{14}$$

$$\Delta\left[\frac{B^2}{8\pi}\right] = \frac{\tilde{\rho}\tilde{U}_f\tilde{\alpha}_s}{\tilde{a}}(\tilde{U}_s^2 - \tilde{a}^2)(\tilde{\alpha}_5 + \tilde{\alpha}_3) + \tilde{\rho}\tilde{\alpha}_f(\tilde{U}_f^2 - \tilde{a}^2)(\tilde{\alpha}_7 + \tilde{\alpha}_1), \tag{15}$$

which will be used later.

$$\begin{aligned}\Delta[\rho V_x] = &\frac{\tilde{\rho}\tilde{U}_f\tilde{\alpha}_s}{\tilde{a}}\tilde{V}_x(\tilde{\alpha}_5 + \tilde{\alpha}_3) + \tilde{\rho}\tilde{U}_A\tilde{\alpha}_s(\tilde{\alpha}_5 - \tilde{\alpha}_3) + \tilde{\rho}\tilde{\alpha}_f\tilde{V}_x(\tilde{\alpha}_7 + \tilde{\alpha}_1)\\ &+ \tilde{\rho}\tilde{V}_x\tilde{\alpha}_4 + \tilde{\rho}\tilde{\alpha}_f\tilde{U}_f(\tilde{\alpha}_7 - \tilde{\alpha}_1),\end{aligned} \tag{16}$$

$$\Delta\left[P+\rho V_x^2+\frac{B_\perp^2}{8\pi}\right]=\tilde{\rho}\tilde{V}_x^2\tilde{\alpha}_4+\frac{\tilde{\rho}\tilde{U}_f\tilde{\alpha}_s}{\tilde{a}}(\tilde{V}_x^2+\tilde{U}_s^2)(\tilde{\alpha}_5+\tilde{\alpha}_3)$$
$$+2\tilde{\rho}\tilde{U}_A\tilde{\alpha}_s\tilde{V}_x(\tilde{\alpha}_5-\tilde{\alpha}_3)+\tilde{\rho}\tilde{\alpha}_f(\tilde{V}_x^2+\tilde{U}_f^2)(\tilde{\alpha}_7+\tilde{\alpha}_1)$$
$$+2\tilde{\rho}\tilde{\alpha}_f\tilde{U}_f\tilde{V}_x(\tilde{\alpha}_7-\tilde{\alpha}_1), \tag{17}$$

$$\Delta\left[\rho V_xV_y-\frac{B_xB_y}{4\pi}\right]=\tilde{\rho}\tilde{V}_x\tilde{V}_y\tilde{\alpha}_4-\frac{\tilde{\beta}_z}{4\pi}\tilde{V}_x(\tilde{\alpha}_6-\tilde{\alpha}_2)-\frac{\tilde{\beta}_z}{4\pi}\tilde{U}_A(\tilde{\alpha}_6+\tilde{\alpha}_2)$$
$$+\left(\frac{\tilde{\rho}\tilde{U}_f}{\tilde{a}}\tilde{\alpha}_s\tilde{V}_xV_y+\tilde{\rho}\tilde{U}_f\tilde{\alpha}_f\tilde{\beta}_yS\right)(\tilde{\alpha}_5+\tilde{\alpha}_3)$$
$$+(\tilde{\rho}\tilde{U}_A\tilde{\alpha}_s\tilde{V}_y+\tilde{\rho}\tilde{U}_f\tilde{\alpha}_f\tilde{\beta}_y\tilde{V}_xS)(\tilde{\alpha}_5-\tilde{\alpha}_3)$$
$$+(\tilde{\rho}\tilde{\alpha}_f\tilde{V}_x\tilde{V}_y-\tilde{\rho}\tilde{U}_A\tilde{\alpha}_s\tilde{\beta}_y\tilde{U}_f)(\tilde{\alpha}_7+\tilde{\alpha}_1)$$
$$+(\tilde{\rho}\tilde{\alpha}_f\tilde{V}_y\tilde{U}_f-\tilde{\rho}\tilde{U}_A\tilde{\alpha}_s\tilde{\beta}_yV_xS)(\tilde{\alpha}_7-\tilde{\alpha}_1), \tag{18}$$

$$\Delta\left[\rho V_xV_z-\frac{B_xB_z}{4\pi}\right]=\tilde{\rho}\tilde{V}_x\tilde{V}_z\tilde{\alpha}_4+\frac{\tilde{\beta}_y}{4\pi}\tilde{V}_x(\tilde{\alpha}_6-\tilde{\alpha}_2)-\frac{\tilde{\beta}_y}{4\pi}\tilde{U}_A(\tilde{\alpha}_6+\tilde{\alpha}_2)$$
$$-\left(\frac{\tilde{\rho}\tilde{U}_f}{\tilde{a}}\tilde{\alpha}_s\tilde{V}_x\tilde{V}_z+\tilde{\rho}\tilde{U}_f\tilde{\alpha}_f\tilde{\beta}_zS\right)(\tilde{\alpha}_5+\tilde{\alpha}_3)$$
$$+(\tilde{\rho}\tilde{U}_A\tilde{\alpha}_s\tilde{V}_z+\tilde{\rho}\tilde{U}_f\tilde{\alpha}_f\tilde{\beta}_z\tilde{V}_xS)(\tilde{\alpha}_5-\tilde{\alpha}_3)$$
$$+(\tilde{\rho}\tilde{\alpha}_f\tilde{V}_x\tilde{V}_z-\tilde{\rho}\tilde{U}_A\tilde{\alpha}_s\tilde{\beta}_z\tilde{U}_f)(\tilde{\alpha}_7+\tilde{\alpha}_1)$$
$$+(\tilde{\rho}\tilde{\alpha}_f\tilde{V}_z\tilde{U}_f-\tilde{\rho}\tilde{U}_A\tilde{\alpha}_s\tilde{\beta}_zV_xS)(\tilde{\alpha}_7-\tilde{\alpha}_1), \tag{19}$$

$$\Delta[V_xB_y-V_yB_x]=\frac{\tilde{\beta}_zS}{\sqrt{(4\pi\tilde{\rho})}}\tilde{V}_x(\tilde{\alpha}_6+\tilde{\alpha}_2)-\frac{\tilde{\beta}_zS}{\sqrt{(4\pi\tilde{\rho})}}\tilde{U}_A(\tilde{\alpha}_6-\tilde{\alpha}_2)$$
$$+\tilde{a}\tilde{\beta}_y\tilde{\alpha}_f\sqrt{(4\pi\tilde{\rho})}\tilde{V}_x(\tilde{\alpha}_5+\tilde{\alpha}_3)-\tilde{a}\tilde{\beta}_y\tilde{\alpha}_f\sqrt{(4\pi\tilde{\rho})}\tilde{U}_s(\tilde{\alpha}_5-\tilde{\alpha}_3)$$
$$+\tilde{U}_f\tilde{\beta}_y\tilde{\alpha}_s\sqrt{(4\pi\tilde{\rho})}\tilde{V}_x(\tilde{\alpha}_7+\tilde{\alpha}_1)+\tilde{U}_f\tilde{\beta}_y\tilde{\alpha}_s\sqrt{(4\pi\tilde{\rho})}\tilde{U}_f(\tilde{\alpha}_7-\tilde{\alpha}_1), \tag{20}$$

$$\Delta[V_xB_z-V_zB_x]=-\frac{\tilde{\beta}_yS}{\sqrt{(4\pi\tilde{\rho})}}\tilde{V}_x(\tilde{\alpha}_6+\tilde{\alpha}_2)+\frac{\tilde{\beta}_yS}{\sqrt{(4\pi\tilde{\rho})}}\tilde{U}_A(\tilde{\alpha}_6-\tilde{\alpha}_2)$$
$$+\tilde{a}\tilde{\beta}_z\tilde{\alpha}_f\sqrt{(4\pi\tilde{\rho})}\tilde{V}_x(\tilde{\alpha}_5+\tilde{\alpha}_3)-\tilde{a}\tilde{\beta}_z\tilde{\alpha}_f\sqrt{(4\pi\tilde{\rho})}\tilde{U}_s(\tilde{\alpha}_5-\tilde{\alpha}_3)$$
$$+\tilde{U}_f\tilde{\beta}_z\tilde{\alpha}_s\sqrt{(4\pi\tilde{\rho})}\tilde{V}_x(\tilde{\alpha}_7+\tilde{\alpha}_1)+\tilde{U}_f\tilde{\beta}_z\tilde{\alpha}_s\sqrt{(4\pi\tilde{\rho})}\tilde{U}_f(\tilde{\alpha}_7-\tilde{\alpha}_1), \tag{21}$$

$$\Delta\left[(E_\perp+P_\perp^*)V_x-\frac{B_x}{4\pi}\vec{v}_\perp\cdot\vec{v}_\perp\right]=\tilde{\rho}\,\frac{\tilde{V}^2}{2}\tilde{V}_x\tilde{\alpha}_4+\frac{\tilde{\beta}_y\tilde{V}_z-\tilde{\beta}_z\tilde{V}_y}{4\pi}\tilde{V}_x(\tilde{\alpha}_6-\tilde{\alpha}_2)$$
$$+\frac{\tilde{\beta}_y\tilde{V}_z-\tilde{\beta}_z\tilde{V}_y}{4\pi}\tilde{U}_A(\tilde{\alpha}_6+\tilde{\alpha}_2)\cdots, \tag{22}$$

where $\gamma'=(\gamma-2)/(\gamma-1)$ and $S=\mathrm{Sign}(\tilde{B}_x)$. In addition, $\tilde{\beta}_{y,z}$ and $\tilde{\alpha}_{s,f}$ are defined by

$$\tilde{\beta}_y=\frac{\tilde{B}_y}{\sqrt{(\tilde{B}_y^2+\tilde{B}_z^2)}},\qquad \tilde{\beta}_z=\frac{\tilde{B}_z}{\sqrt{(\tilde{B}_y^2+\tilde{B}_z^2)}}, \tag{23}$$

$$\tilde{\alpha}_s = \sqrt{\left(\frac{\tilde{U}_f^2 - \tilde{a}^2}{\tilde{U}_f^2 - \tilde{U}_s^2}\right)}, \qquad \tilde{\alpha}_f = \sqrt{\left(\frac{\tilde{U}_f^2 - \tilde{U}_A^2}{\tilde{U}_f^2 - \tilde{U}_s^2}\right)}, \tag{24}$$

where $\tilde{U}_f, \tilde{U}_s$, and $\tilde{U}_A$ are fast, slow and Alfven speeds respectively given by

$$\tilde{U}_f = \sqrt{\{\tfrac{1}{2}[a^{*2} + \sqrt{(a^{*4} - 4\tilde{a}^2\tilde{U}_A^2)}]\}}, \tag{25}$$

$$\tilde{U}_s = \sqrt{\{\tfrac{1}{2}[a^{*2} - \sqrt{(a^{*4} - 4\tilde{a}^2\tilde{U}_A^2)}]\}}, \tag{26}$$

$$\tilde{U}_A = \sqrt{(\tilde{B}_x^2/4\pi\tilde{\rho})}, \tag{27}$$

with $a^{*2} = \tilde{a}^2 + \tilde{B}^2/4\pi\tilde{\rho}$.

Here $\tilde{\beta}_y$ and $\tilde{\beta}_z$ represent the cosine and sine of the rotation angle of the perpendicular magnetic field $\tilde{B}_\perp$ on the y–z plane respectively and $\tilde{\alpha}_s$ and $\tilde{\alpha}_f$ predict how closely the sound and Alfven waves propagate with respect to the fast wave respectively.

Since the MHD equations are not strictly hyperbolic, there are some points at which some of the eigenvectors may become degenerate and some of the parameters cannot be determined accurately. For instance, $\tilde{\beta}_y$ and $\tilde{\beta}_z$ become indeterminate as $\tilde{B}_\perp$ approaches zero. This is the limit which consists of three degeneracies depending on the relative values of the sound and Alfven waves. If $U_A \gg a$, fast and Alfven waves; if $U_A \ll a$, slow and Alfven waves; and if $U_A = a$, fast, Alfven, and slow waves travel with almost the same speed. It is suggested in References 7 and 8 that one may take $\tilde{\beta}_y = \tilde{\beta}_z = 1/\sqrt{2}$ whenever $\tilde{B}_\perp$ gets too small. Even though this arbitrary fix preserves the orthonormality of the eigenvectors, it is not unique. For example, checking the relative magnitudes of $\tilde{B}_y$ and $\tilde{B}_z$ near such a point and assigning different waves to $\tilde{\beta}_y$ and $\tilde{\beta}_z$ such that the square sum of them becomes unity produces another fix. Yet another fix was introduced by Zachary *et al.*,[13] who separated and handled these three situations by means of structure coefficients.

Another degeneracy point occurs when both $\tilde{B}_x$ vanishes and $\tilde{B}_\perp$ changes sign (or $\tilde{B}$ goes to zero). In this limit Alfven, slow and sound waves travel with the same speed. This situation may lead to a strong sonic point and hence a non-physical expansion shock in the numerical solutions if it is not handled properly. In this paper a new fix of this sonic point is introduced. The idea of this sonic fix was originally introduced by Roe[14] for the Euler equations and was extended to MHD by Aslan.[10]

It is shown that the R–H conditions given by equations (4) and (5) produce 14 equations to be solved for seven primitive state averages (*i.e.* $\tilde{\rho}, \tilde{V}_x, \tilde{V}_y, \tilde{V}_z, \tilde{B}_y, \tilde{B}_z$, and $\tilde{p}$). In what follows, the procedure for obtaining these averages is summarized.

Using equation (16) in equation (17) and considering equations (8), (14) and (15), one obtains

$$\Delta[P + \rho V_x^2] = \tilde{V}_x\Delta[\rho V_x] + \rho\tilde{V}_x\Delta[V_x]. \tag{28}$$

Using equation (7) and (8) in equation (16) gives

$$\Delta[\rho V_x] = \tilde{V}_x\Delta[\rho] + \tilde{\rho}\Delta[V_x]. \tag{29}$$

Assume now that the jump around the averaged state $\tilde{U}$ is taken as $\Delta[U] = U^R - U^L$, where superscripts R and L denote the right and left states around the interface respectively. In this case, with the help of equations (14) and (29), equation (28) leads to

$$\tilde{V}_x = \frac{\sqrt{\rho^R}V_x^R + \sqrt{\rho^L}V_x^L}{\sqrt{\rho^R} + \sqrt{\rho^L}}. \tag{30}$$

Using this in equation (29) results in

$$\tilde{\rho} = \sqrt{(\rho^R\rho^L)}. \tag{31}$$

Multiplying equation (7) by V_xV_y and equation (8) and (9) by ρV_x and ρV_y respectively, it is easy to see that equation (18) produces

$$\Delta[\rho V_xV_y] = \tilde{V}_x\tilde{V}_y\Delta[\rho] + \tilde{\rho}\tilde{V}_y\Delta[V_x] + \tilde{\rho}\tilde{V}_x\Delta[V_y]. \tag{32}$$

Applying the same procedure to equation (19) results in

$$\Delta[\rho V_xV_z] = \tilde{V}_x\tilde{V}_z\Delta[\rho] + \tilde{\rho}\tilde{V}_z\Delta[V_x] + \tilde{\rho}\tilde{V}_x\Delta[V_z]. \tag{33}$$

Multiplying equation (11) and (12) by $\tilde{B}_x$, one can see that equations (18) and (19) also produce

$$\Delta[B_xB_{y,z}] = \tilde{B}_x\Delta B_{y,z}, \tag{34}$$

which will be used later. It is trivial to show that equation (7) and (9) and equation (32) and (33) lead to

$$\Delta[\rho V_{y,z}] = \tilde{V}_{y,z}\Delta[\rho] + \tilde{\rho}\Delta[V_{y,z}]. \tag{35}$$

From equation (35) the following averages for V_y and V_z are obtained:

$$\tilde{V}_y = \frac{\sqrt{\rho^R}V_y^R + \sqrt{\rho^L}V_y^L}{\sqrt{\rho^R} + \sqrt{\rho^L}}, \qquad \tilde{V}_z = \frac{\sqrt{\rho^R}V_z^R + \sqrt{\rho^L}V_z^L}{\sqrt{\rho^R} + \sqrt{\rho^L}}. \tag{36}$$

Notice that the first, third and fifth terms on the right-hand side of equation (20) and (21) are $\tilde{V}_x\Delta[B_y]$ and $\tilde{V}_x\Delta[B_z]$ respectively. Notice also that, using the identities

$$\tilde{U}_A\tilde{a} = \tilde{U}_f\tilde{U}_s, \qquad \tilde{U}_f\frac{\tilde{\alpha}_f}{\tilde{\alpha}_s}\tilde{U}_\perp = \tilde{U}_f^2 - \tilde{U}_A^2, \tag{37}$$

where $\tilde{U}_\perp = \sqrt{(B_\perp^2/4\pi\rho)}$, the rest of these terms lead to $\tilde{B}_{y,z}\Delta[V_x] - \tilde{B}_x\Delta[V_{y,z}]$. In this case equations (20) and (21) turn into

$$\Delta[V_xB_{y,z}] - \Delta[V_{y,z}B_x] = \tilde{V}_x\Delta[B_{y,z}] + \tilde{B}_{y,z}\Delta[V_x] - \tilde{B}_x\Delta[V_{y,z}], \tag{38}$$

which splits into (by means of equations (8)–(12))

$$\Delta[V_xB_{y,z}] = \tilde{V}_x\Delta[B_{y,z}] + \tilde{B}_{y,z}\Delta[V_x], \tag{39}$$

$$\Delta[V_{y,z}B_x] = \tilde{B}_x\Delta[V_{y,z}]. \tag{40}$$

It is easy to show that equation (39) results in the following amazingly simple averages for B_y and B_z:

$$\tilde{B}_y = \frac{\sqrt{\rho^L}B_y^R + \sqrt{\rho^R}B_y^L}{\sqrt{\rho^R} + \sqrt{\rho^L}}, \qquad \tilde{B}_z = \frac{\sqrt{\rho^L}B_z^R + \sqrt{\rho^R}B_z^L}{\sqrt{\rho^R} + \sqrt{\rho^L}}. \tag{41}$$

It is easy to see that equations (34) and (40) are satisfied only when $\tilde{B}_x = B_x^R = B_x^R$, which states that $\Delta B_x = 0$. If this condition does not hold, the averages for magnetic field and pressure do not exist even though the averages for density and velocity still hold.

Taking advantage of the results found so far, using the expressions

$$\tilde{\alpha}_s^2 + \frac{\tilde{a}^2}{\tilde{U}_f^2}\tilde{\alpha}_f^2 = 1, \qquad \tilde{U}_s^2 = \tilde{a}^2 = -\frac{\tilde{a}^2\tilde{\alpha}_f}{\tilde{U}_f\tilde{\alpha}_s}\tilde{U}_\perp,$$

$$\tilde{U}_f^2 - \tilde{a}^2 = \frac{\tilde{U}_f\tilde{\alpha}_s}{\tilde{\alpha}_f}\tilde{U}_\perp, \qquad \tilde{U}_f^2 - \tilde{U}_s^2 = \frac{\tilde{U}_f}{\tilde{\alpha}_f\tilde{\alpha}_s}\tilde{U}_\perp,$$

and going through tedious but trivial derivations, equation (22) leads to

$$\Delta[V_x P] = \tilde{V}_x \Delta[P] + \tilde{P}\Delta[V_x], \tag{42}$$

which produces the simple equation for the average pressure

$$\tilde{P} = \frac{\sqrt{\rho^{\mathrm{L}}}P^{\mathrm{R}} + \sqrt{\rho^{\mathrm{R}}}P^{\mathrm{L}}}{\sqrt{\rho^{\mathrm{R}}} + \sqrt{\rho^{\mathrm{L}}}}. \tag{43}$$

Therefore all 14 equations given above are utilized such that the averages for the seven primitive states will satisfy all these equations only if B_x is constant in space.

If B_x is not constant (along with equations (31), (32) and (36)), one can take the following averages of magnetic field and pressure:

$$\tilde{\vec{B}} = \frac{\vec{B}^{\mathrm{L}} + \vec{B}^{\mathrm{R}}}{2}, \qquad \tilde{P} = \frac{P^{\mathrm{L}} + P^{\mathrm{R}}}{2}. \tag{44}$$

In this case, as Brio and Wu[7] remarked, the stationary discontinuities will no longer be the steady solutions of the scheme but will still be resolved within only a few grid points.

4. NUMERICAL INTEGRATION WITH FLUCTUATION SPLITTING

Considering a uniform grid and denoting the state vector by U_i^n at time $t = n\Delta t$ and location $x = x_0 + i\Delta x$, equation (1) is rearranged to read

$$\frac{U_p^{n+1} - U_p^n}{\Delta t} + \frac{F_{i+1}^n - F_i^n - \Delta x S_x}{\Delta x} = 0. \tag{45}$$

Taking $\Delta F = F_{i+1}^n - F_i^n$ and using the decompositions given in equations (4)–(6), equation (45) becomes

$$U_p^{n+1} = U_p^n - \frac{\Delta t}{\Delta x}\sum_k (\tilde{\lambda}_k \tilde{\alpha}_k + \tilde{\beta}_k)\tilde{r}_k. \tag{46}$$

In the fluctuation approach[6] one evaluates the fluctuation for each interval $[x_i, x_{i+1}]$ by

$$\phi_{i+1/2}^k = (\tilde{\lambda}_k \tilde{\alpha}_k + \tilde{\beta}_k)\tilde{r}_k \tag{47}$$

and the total signal by $\Phi_{i+1/2}^k = (\Delta t/\Delta x)\phi_{i+1/2}^k$. In this equation (46) turns into

$$U_p^{n+1} = U_p^n - \sum_k \Phi_{i+1/2}^k, \tag{48}$$

where p may be i or $i+1$ depending on σ_k, the sign of λ_k.

For each kth field, subtracting $\Phi_{i+1/2}^k$ from $U_{i+1/2+\sigma_k/2}$ therefore completes an upwind, first-order, conservative and local bounding scheme. A Lax–Wendroff-type, second-order-limited, conservative scheme is completed by adding

$$\Psi(b_u/b_{i+1/2}^k)b_{i+1/2}^k \tag{49}$$

to $U_{i+1/2+\sigma_k/2}$ and subtracting it from $U_{i+1/2-\sigma_k/2}$. Here Ψ is the flux limiter (required for local boundness) and

$$b_{i+1/2}^k = \tfrac{1}{2}(1 - |\tilde{\nu}|)\Phi_{i+1/2}^k, \qquad b_{\mathrm{u}} = \tfrac{1}{2}[(1 - \sigma_k)b_{i+3/2}^k + (1 + \sigma_k)b_{i+1/2}^k], \tag{50}$$

where $\tilde{\nu}_k = (\Delta t/\Delta x)\tilde{\lambda}_k$ is the Courant number for the kth field.

It is noted that as the limiters[15] become more compressive (e.g. Roe's Superbee), the shocks and discontinuities become rather sharp but the post-slow-shock oscillations increase. However, less compressive limiters (e.g. van Leer's or van Albada's limiter) produce less oscillations but less sharp discontinuities. Therefore it is obvious that the accuracy of the solutions depends on the type of limiter used. This is an issue on which more investigation must be done.

5. NEW SONIC FIX

In order to understand the new sonic fix, equation (1) is written as

$$U_t + A(U)U_x = S_x, \tag{51}$$

where $A(U)$ is the flux Jacobian. Differentiate this equation with respect to x and multiply by the left eigenvector of $A(U)$ to get

$$l \cdot [U_{xt} + A_x U_x + A U_{xx} - S_x] = 0. \tag{52}$$

Since $l_k A = \lambda_k l$ at the sonic point where λ_k *vanishes*, the above equation becomes (for the kth field)

$$l_k U_{xt} = l_k[-A_x U_x + S_x]. \tag{53}$$

Here the term $l_k U_{xt}$ can be defined as a measure of the rate at which the wave of the sonic family is decaying.[14] Let δU_{L}^* and δU_{R}^* be the proper changes in the left and right cells respectively after U^* is obtained by any method explicitly from U^n (*i.e.* $\delta U_{\mathrm{L,R}}^* = U_{\mathrm{L,R}}^n$). Writing

$$l_k U_{xt} = l_k \frac{1}{\Delta t}\left[\frac{U_{\mathrm{R}}^* - U_{\mathrm{L}}^*}{\Delta x} - \frac{U_{\mathrm{R}}^n - U_{\mathrm{L}}^n}{\Delta x}\right]_k \tag{54}$$

or

$$l_k U_{xt} = \frac{1}{\Delta x \Delta t} l_k[\delta U_{\mathrm{R}}^* - \delta U_{\mathrm{L}}^*], \tag{55}$$

equation (53) becomes

$$l_k[\delta U_{\mathrm{R}}^* = \delta U_{\mathrm{L}}^*] = \Delta x \Delta t l_k[-A_x U_x + S_x]_k. \tag{56}$$

In order for this proper change to be equal to the numerical change $\delta U_{\mathrm{R}} = \delta U_{\mathrm{L}}$, one needs

$$l_k[\delta U_{\mathrm{R}}^* + \delta U_{\mathrm{L}}^*] = l_k[\delta U_{\mathrm{R}} + \delta U_{\mathrm{L}}] \tag{57}$$

for conservation. It is easy to see that equation (56) and (57) now lead to

$$l_k[\delta U_{\mathrm{L}}^* - \delta U_{\mathrm{L}}] = \kappa_k, \tag{58}$$

$$l_k[\delta U_{\mathrm{R}}^* - \delta U_{\mathrm{R}}] = \kappa_k, \tag{59}$$

where $\kappa_k = \frac{1}{2} l_k[\delta U_{\mathrm{R}} - \delta U_{\mathrm{L}} + (A_x U_x - S_x)\Delta x \Delta t]$. Premultiplying equations (58) and (59) by r^k and using $l_k \cdot r^k = 1$ leads to the numerical error on the left and right states after U^* is obtained:

$$\varepsilon_L \equiv \delta U_{\mathrm{L}}^* - \delta U_{\mathrm{L}} = \kappa_k r^k, \tag{60}$$

$$\varepsilon_{\mathrm{R}} \equiv \delta U_{\mathrm{R}}^* - \delta U_{\mathrm{R}} = \kappa_k r^k, \tag{61}$$

Therefore adding $\kappa_k r^k$ to U_{L}^* and subtracting it from U_{R}^* will cancel these errors. The procedure for fixing the sonic point therefore begins by first detecting the sonic point due to the kth field after the

new state U^* is obtained from U^n. Then the corrected states at time level $n+1$ are obtained via

$$\vec{U}_{i+1}^{n+1} = \vec{U}_{i+1}^{*} + \kappa_k \vec{r}_k, \tag{62}$$

$$\vec{U}_{i}^{n+1} = \vec{U}_{i}^{*} - \kappa_k \vec{r}_k. \tag{63}$$

6. NUMERICAL RESULTS

The scheme described in previous sections is applied to Sod's shock tube problem[16] as a check on the coding as the magnetic field vanishes. The initial data for this problem are given by $\rho_L = 1{\cdot}0$, $\rho_R = 0{\cdot}125$, $P_L = 1{\cdot}0$, $P_R = 0{\cdot}1$ and $\vec{V} = 0$, $\vec{B} = 0$ for an ideal gas with $\gamma = 1{\cdot}4$. The exact solution consists of a shock and contact discontinuity moving to the right and a rarefaction wave moving to the left. A uniform mesh of 100 points with $\Delta t/\Delta x = 0{\cdot}411$ and the fluctuation approach with the Superbee limiter are used and the results are plotted after 35 time steps (at $t = 0{\cdot}144$) in Figures 1(a) and 1(b). Note that the labels (rf−, c, s+) on these figures correspond to rarefaction fan, contact and slow shock waves respectively. These satisfactory results display very sharp shock and contact discontinuities and are very much better than those obtained by Sod.[16]

The next test problem is an MHD version of Sod's shock tube problem originally introduced by Brio and Wu.[7] In this case a uniform grid of 800 points is used together with $\Delta t/\Delta x = 0{\cdot}2$ and an adiabatic index $\gamma = 2{\cdot}0$. The initial condition is given by

$$W_{\mathrm{L}} = [1, 0, 0, 0, 0, \sqrt{(4\pi)}, 0, 1], \qquad W_{\mathrm{R}} = [0{\cdot}125, 0, 0, 0, 0, -\sqrt{(4\pi)}, 0, 0{\cdot}1]. \tag{64}$$

The numerical results obtained from the second-order scheme with full Roe averaging and the Superbee limiter for the linear (entropy, Alfven) and van Leer's limiter for the non-linear (slow, fast) fields are shown in Figure 2. Note that in obtaining for these results, the limiter was turned off at the degeneracy point to create a pointwise dissipation, which is required for non-strictly hyperbolic systems.[17]

The initial jump $B_\perp$ creates a degeneracy point ($B_\perp \approx 0$) at which β_y and β_z must be redefined. In obtaining these results, the degeneracy point is flagged whenever $B_\perp$ is smaller than a certain value and β_y and β_z are set to $1/\sqrt{2}$ at this point. Various numerical experiments showed that choosing this value between 0·01 and 0·3 provided a good fix, while the flux showed almost no change within this range. The arbitrariness in choosing a small parameter to detect where the magnetic field vanishes and the assignment of arbitrary values to β_y and β_z in this limit must be studied further.

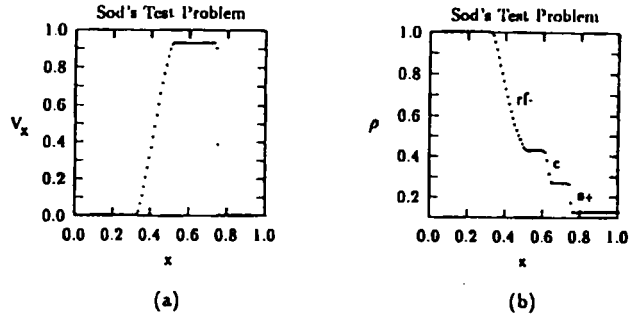

Figure 1. Numerical solutions for Sod's shock tube problem. The labels (rf−, c, s+) denote rarefaction fan, contact and slow shock waves respectively

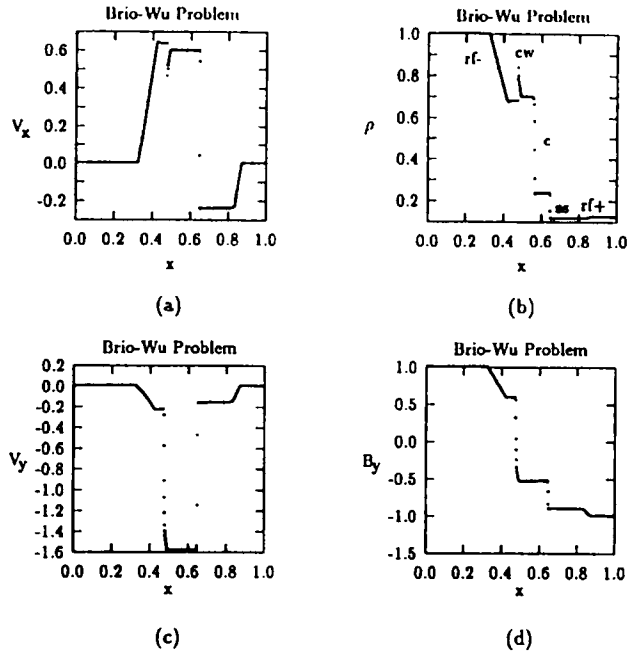

Figure 2. Numerical solutions for Brio and Wu's first test problem. The results are obtained at $t = 0{\cdot}1$ with $\Delta t/\Delta x = 0{\cdot}2$. The labels (rf−, cw, c, ss, rf+) denote left-moving rarefaction, compound, contact, slow shock and right-moving rarefaction waves respectively

For the last ten problem the same grid is used with $\Delta t/\Delta x = 0{\cdot}2$. The initial condition is given by

$$W_L = [1, 0, 0, 0, 0, \sqrt{(4\pi)}, 0, 1000], \qquad W_R = [0{\cdot}125, 0, 0, 0, 0, = \sqrt{(4\pi)}, 0, 0{\cdot}1], \tag{65}$$

with an adiabatic index $\gamma = 5/3$. Notice the large initial pressure jump at the interface. In Roe's method this jump causes a strong (unphysical) expansion shock if no fix is done at the sonic point. To eliminate this expansion shock, the new sonic fix described in Section 5 is used.[10] In order to show the effects of the new sonic fix with Roe averaging and different limiters, V_x plots for various cases are shown in Figure 3. Figure 3(a) is obtained with arithmetic averaging, the Superbee limiter and no sonic fix. As can be seen, there exists an unphysical expansion shock (labelled 'es' on the figure) and an overshoot on the rarefaction fan and post-shock oscillations. Figure 3(b) shows the results after the new sonic fix is used. It can be seen that the expansion shock is totally eliminated, but this fix does not handle the overshoot and post-shock oscillations. Figure 3(c) is obtained using full Roe averaging. The result is that the overshoot and most of the post-shock oscillations are eliminated. Turning off the limiter at the shock and using the less compressive van Leer limiter leads to the excellent results shown in Figures 3(d) and 4.

During the numerical experiments the average execution time per grid point was found to be within 0·1–0·25 s in real time on a personal computer (486, 66 MHz, 16 Mbyte RAM).

7. CONCLUSIONS

In this paper an explicit, second-order Godunov-type method based on the fluctuation approach is presented for the solution of one-dimensional problems in ideal magnetohydrodynamics (MHD). The numerical results show that the method is sufficiently robust and can handle degeneracies and sonic

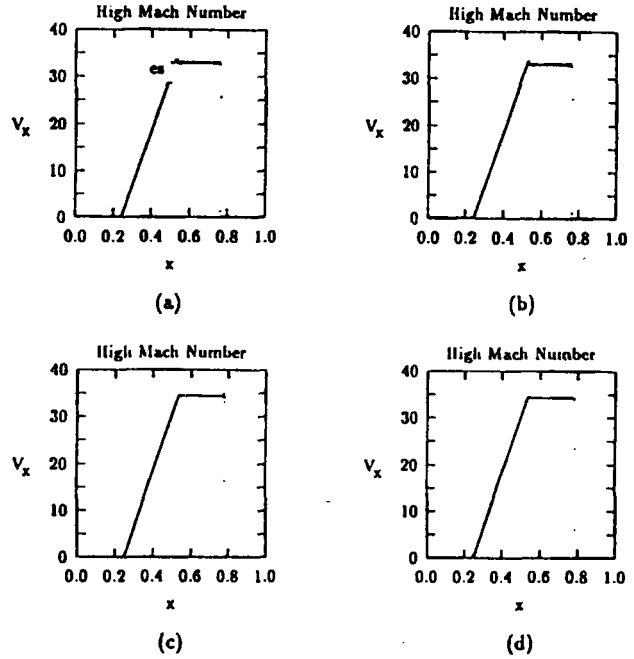

Figure 3. Numerical solutions for high-Mach-number problem of Brio and Wu, showing from (a) to (d) how to eliminate the expansion shock and the overshoot on the rarefaction fan and post-shock oscillations

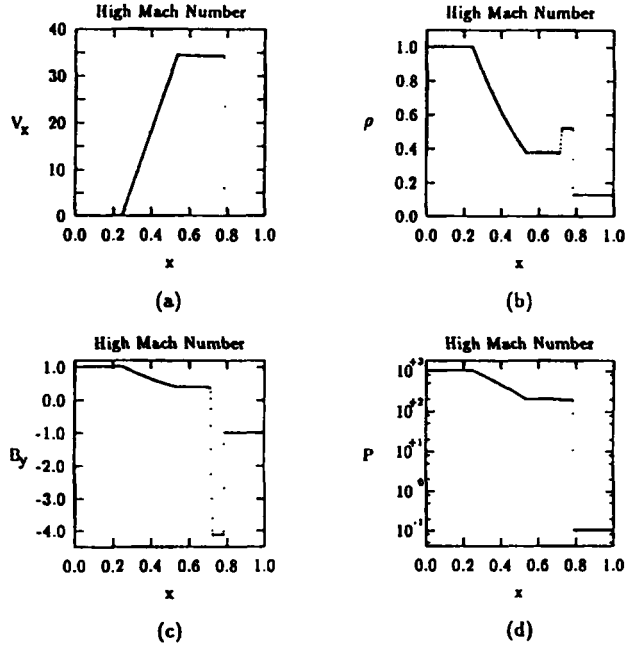

Figure 4. Results for Brio and Wu's high-Mach-number problem obtained with the second-order fluctuation approach, Roe averaging, the new sonic fix and van Leer's limiter, which is turned off at the shock

points very efficiently. The new sonic fix introduced in this paper provides a thorough treatment of the sonic points in MHD and requires no structure coefficients or any kind of artificial viscosity. The new Roe averaging is also proven to work very well for any value of the adiabatic index γ. The results presented in this paper are in excellent agreement with those obtained earlier and create sharper discontinuities and shocks. The effect of viscosity at the degenerate points and a two-dimensional extension of the method are being investigated and will be the subject of subsequent publications.

ACKNOWLEDGEMENT

I appreciate the numerous discussions with Phillip Roe, who has always been a great source of inspiration.

REFERENCES

1. B. van Leer, *J. Comput. Phys.*, **23**, 276 (1987).
2. P. L. Roe, *J. Comput. Phys.* **43**, 357 (1981).
3. P. R. Woodward and P. Colella, *J. Comput. Phys.*, **54**, 115 (1984).
4. P. K. Sweby, *Numerical Analysis Report 6/82*, University of Reading, 1982.
5. A. Harten, *J. Comput. Phys.*, **49**, 357 (1983).
6. P. L. Roe and M. J. Baines, *Proc. 4th GAMM Conf. on Numerical Methods in Fluid Mechanics*, Vieweg, Braunschweig, 1982.
7. M. Brio and C. C. Wu, *J. Comput. Phys.*, **75**, 400 (1988).
8. A. Zachary and P. Colella, *J. Comput. Phys.*, **99**, 4463 (1992).
9. Bell, Colella and Trangenstein.
10. N. Aslan, *Ph.D. Thesis*, University of Michigan, 1993.
11. P. L. Roe and J. Pike, in R. Glowinski and J.-L. Lions (eds), *Computing Methods in Applied Science and Engineering VI*, North-Holland, Amsterdam, 1984, p. 499.
12. P. Glaister, *Numerical Analysis Report 11/86*, University of Reading, 1986.
13. A. Zachary, A. Malagoli and P. Colella, *SIAM J. Sci. Stat. Comput.*, in press.
14. P. L. Roe, *SIAM J. Sci. Stat. Comput.*, **13**, 611 (1992).
15. C. Hirsch. *Numerical Computation of Internal and External Flows*, Wiley, Chichester, 1991.
16. G. A. Sod, *J. Comput. Phys.*, **27**, 1 (1978).
17. H. Freistühler and E. B. Pitman, *J. Comput. Phys.*, **100**, 306 (1992).